

Topological Phase Transition in Sliding Bilayer Graphene

Young-Woo Son,^{1,*} Seon-Myeong Choi,² Yoon Pyo Hong,¹ Sungjong Woo,¹ and Seung-Hoon Jhi^{2,3,†}

¹Korea Institute for Advanced Study, Seoul 130-722, Korea.

²Department of Physics, Pohang University of Science and Technology, Pohang 790-784, Korea.

³Division of Advanced Materials Science, Pohang University of Science and Technology, Pohang 790-784, Korea.

We demonstrate theoretically that the topology of energy bands and Fermi surface in bilayer graphene undergoes a very sensitive transition when extremely tiny lateral interlayer shift occurs in arbitrary directions. The phenomenon originates from a generation of effective non-Abelian vector potential in Dirac Hamiltonian by the sliding motions. The characteristics of the transition such as pair annihilations of massless Dirac fermions are dictated by the sliding direction owing to a unique interplay between the effective non-Abelian gauge fields and Berry's phases associated with massless electrons. The transition manifests itself in various measurable quantities such as anomalous density of states, minimal conductivity, and distinct Landau level spectrum.

PACS numbers: 73.22.Pr, 71.20.-b, 81.05.ue, 61.48.Gh

Changes in the topology of Fermi surfaces known as Lifshitz transition [1] alter physical properties of metals significantly [1–3]. Though such an electronic topological transition (ETT) has been pursued in various materials, its realization requires large external perturbations such as alloying or applying high pressure that hinder clear detections of the transition [1–4]. Recent progress in measuring low energy electronic structures of bilayer graphene (BLG) [5–7] provides a new opportunity to explore the ETT because of its unique electronic structures and because of possible noninvasive control of chemical potential of the system [8]. In BLG, two coupled hexagonal lattices of carbon atoms are arranged according to Bernal stacking [9–14]. Since electrons in a single layer graphene (SLG) behave as relativistic massless fermions [14], BLG provides a unique playground to control interactions between relativistic particles coupled with relative mechanical motions of two layers. Hence, the effects of rotational stacking fault on physical properties of BLG have been studied extensively [6, 15–17]: however, the effect of sliding one layer with respect to the other has not. This mechanical motion is important because the interactions between the two layers are sensitive to the deviation from Bernal stacking [15–17] and extremely small sliding will change its low energy electronic structures significantly.

In this paper, we predict the topological phase transition in energy bands and Fermi surfaces of BLG when sliding motion occurs. It is demonstrated that peculiar coupling between the effective gauge fields with $SU(4)$ symmetry generated by sliding motions and Berry's phase of massless Dirac fermions play a crucial role to change the topology of low energy bands of BLG. They give rise to either pair annihilations of massless Dirac fermions or generations of fermions by absorbing fermions with topological charges, depending on sliding directions. This will offer new opportunities to realize the ETT driven by non-Abelian gauge fields with gentle maneuverable mechanical operations.

Our study of electronic structures of sliding BLG is based on the *ab initio* density functional method [18] within the generalized gradient approximation [19]. A semi-empirical correction of van der Waals force [20, 21] to the approximation is done to obtain the interlayer distance and its binding energy correctly. We also describe the low energy properties of BLG by using an effective field theory with hopping interactions between carbon atoms (Fig. 1). When BLG is in Bernal stacking, the interlayer distance is calculated to be 3.35 Å and its binding energy to be 38.76 meV/atom in good agreement with previous calculations and experiment data [21]. With sliding, we find that the binding energy decreases and the interlayer distance increases, in agreement with a previous study [22]. We note that the change in the binding energy (< 0.19 meV) and interlayer distance (< 0.01 Å) is quite negligible when the sliding distance is less than 0.14 Å (about 10 % of the bond length, a_c).

Considering the low energy electronic structure of BLG in Bernal stacking, our calculations show, as in previous study, four Dirac cones formed around the Fermi energy (E_F) at four Dirac points (\vec{k}_{Di} , $i = 0, 1, 2, 3$) near around K -point [Fig. 2(a) and 2(b)] [9, 10]. The magnitude of \vec{k}_{Di} ($i = 1, 2, 3$) is about 0.4% of the distance between Γ -to K -point ($\overline{\Gamma K}$) [Fig. 2 (b)]. As the energy moves away from the E_F , the four Dirac cones merge to form three saddle points between the cones [Fig. 2(b)]. The calculation result can also be described by an effective Hamiltonian [9], $\mathcal{H}_{\text{eff}}(\vec{k}) = \hbar v_3 \vec{\tau} \cdot \vec{k} + (\hbar^2 v_0^2 / \gamma_1) (\vec{\tau}^* \cdot \vec{k}) \tau_x (\vec{\tau}^* \cdot \vec{k})$ where $v_\alpha = (3/2) \gamma_\alpha a_c / \hbar$ ($\alpha = 0, 3$), $\hbar \vec{k} = \hbar(k_x, k_y)$ is the crystal momentum from K -point, and $\vec{\tau} = (\tau_x, \tau_y)$ and $\vec{\tau}^*$ are Pauli spin matrices and their complex conjugates (See Fig. 1 for definition of γ_α). Typical estimates are $\gamma_0 \simeq 3$ eV, $\gamma_1 \simeq \gamma_3 \simeq \gamma_0/10$ and $\gamma_4 \simeq \gamma_0/20$ [23]. We will neglect γ_4 and discuss its role later. If we expand the effective Hamiltonian around each \vec{k}_{Di} , we have one isotropic Dirac Hamiltonian, $\mathcal{H}_{D0} = \hbar v_3 \vec{\tau} \cdot \delta \vec{k}_0$ at \vec{k}_{D0} , an anisotropic $\mathcal{H}_{D1} = -\hbar v_3 (\tau_x^* \delta k_{x1} + 3 \tau_y^* \delta k_{y1})$ at \vec{k}_{D1} , and two anisotropic others at \vec{k}_{D2} and \vec{k}_{D3} which can be

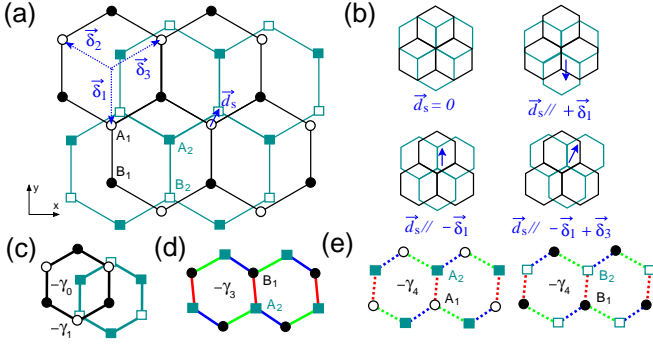


FIG. 1: (a) In the top (black) and bottom layer (green), two sublattices are denoted by empty (A_1) and filled (B_1) circles and by empty (B_2) and filled (A_2) rectangles, respectively. The bottom layer (layer 2) slides with respect to the top (layer 1) by \vec{d}_s . In the top, $\vec{\delta}_1 = (0, -1)a_c$, $\vec{\delta}_2 = (-\frac{\sqrt{3}}{2}, \frac{1}{2})a_c$ and $\vec{\delta}_3 = (\frac{\sqrt{3}}{2}, \frac{1}{2})a_c$. (b) Schematic diagrams for stacking under various sliding directions. (c) The nn intra- and inter-layer hopping parameter, $-\gamma_0$ and $-\gamma_1$. (d) The nnn inter-layer hopping (between B_1 - A_2), $-\gamma_3$ with sliding. (e) The smallest inter-layer hopping (between A_1 - A_2 or B_1 - B_2), $-\gamma_4$ with sliding.

obtained by rotating H_{D1} by $\pm 2\pi/3$ respectively. Here, $\delta \vec{k}_i = (\delta k_{xi}, \delta k_{yi}) = \vec{k} - \vec{k}_{Di}$, ($i = 0, 1, 2, 3$).

We find that the low energy bands of BLG change dramatically when one layer slides with respect to the other in an extremely small amount and in arbitrary directions. Let the bottom layer slide with respect to the top by $\vec{d}_s = (d_x, d_y)$ [Fig. 1(a) and 1(b)]. First, when the bottom layer moves along $\vec{\delta}_1$ direction by 0.028 \AA , i.e., $\vec{d}_s = 0.02\vec{\delta}_1$, only two Dirac cones at \vec{k}_{D2} and \vec{k}_{D3} remain, instead of four cones for BLG without sliding as shown in Fig. 2(c) (See Fig. 1(a) for definition of $\vec{\delta}_i$). The energetic position of the saddle points of the valence band decreases from -1.1 meV to -7.2 meV . When the bottom layer slides further ($\vec{d}_s = 0.1\vec{\delta}_1$), the topology changes again and the saddle point energy significantly decreases to -32.7 meV [Fig. 2(d)]. Second, when the bottom layer moves along the direction opposite to the previous one ($\vec{d}_s = -0.02\vec{\delta}_1$), the low energy bands changes again completely. In this case, the Dirac cone at \vec{k}_{D1} moves along the $-k_x$ direction and an anomalous Dirac cone with sickle-shaped energy contours appears at a new Dirac point instead of three cones [Fig. 2(e)]. If the bottom layer slides further by 0.14 \AA along $-\vec{\delta}_1$ ($\vec{d}_s = -0.1\vec{\delta}_1$), the topology remains the same and the anomalous cone comes to have an anisotropic shape [Fig. 2(f)]. In this case, the saddle point energy decreases to -48.5 meV (almost 500% of pristine one) [Fig. 2(f)]. Finally, when we slide the bottom layer by $0.012(\vec{\delta}_3 - \vec{\delta}_1)$ [Fig. 2(g)] and $0.1(\vec{\delta}_3 - \vec{\delta}_1)$ [Fig. 2(h)], the topological changes are similar to the case for the sliding along $-\vec{\delta}_1$. The saddle point energy for the sliding by $0.1(\vec{\delta}_3 - \vec{\delta}_1)$ decreases dramatically down to -74.0 meV as shown in

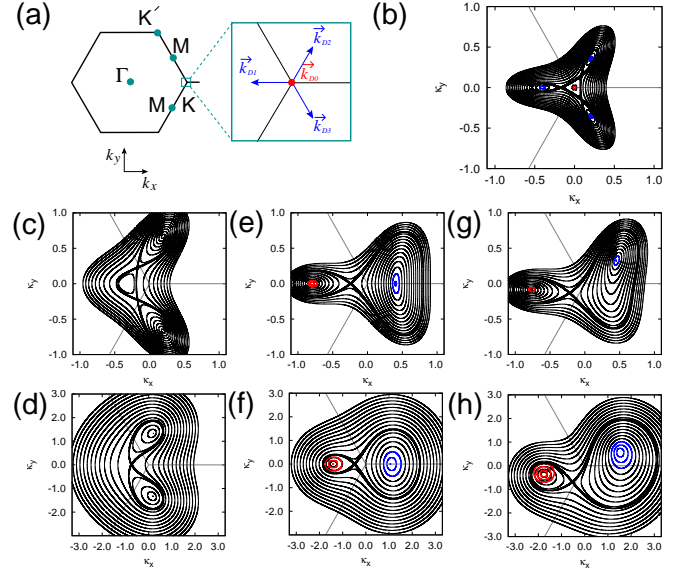


FIG. 2: (a) The small rectangle near around K-point in the first Brillouin zone is enlarged to show the three-fold symmetric vectors $\vec{k}_{D1} = p_D(-1, 0)$, $\vec{k}_{D2} = p_D(1/2, \sqrt{3}/2)$, and $\vec{k}_{D3} = p_D(1/2, -\sqrt{3}/2)$ with respect to $\vec{k}_{D0} = 0$, where $p_D \equiv (2/3a_c)(\gamma_1\gamma_3/\gamma_0^2)$. (b) Energy contour for the valence bands of BLG without sliding. For all panels, $\kappa_x = 100 \times (k_x - \Gamma K)/\Gamma K$ and $\kappa_y = 100 \times k_y/\Gamma K$. The thick contour is an iso-energy ($E = -1.1 \text{ meV}$) curve crossing the three saddle points. The blue (red) contours denote the hole (electron) pockets. Energy contours for the valence band of BLG with sliding $\vec{d}_s =$ (c) $0.02\vec{\delta}_1$, (d) $0.1\vec{\delta}_1$, (e) $-0.02\vec{\delta}_1$, (f) $-0.1\vec{\delta}_1$, (g) $0.012(\vec{\delta}_3 - \vec{\delta}_1)$, and (h) $0.1(\vec{\delta}_3 - \vec{\delta}_1)$. The contour interval is set by 0.5 meV for (a), by 1.0 meV for (c), (e) and (g) and by 10 meV for (d), (f) and (h). The thick contours that cross the saddle points are at $E =$ (c) -7.2 meV , (d) -32.7 meV , (e) -10.8 meV , (f) -48.5 meV , (g) -9.7 meV and (h) -74.0 meV .

Fig. 2(h). After a comprehensive search for the topological changes by the sliding along arbitrary directions (not shown here), we find that the topology of saddle point energy contours is all similar to those shown in Fig. 2(e)-(h) (one crossing point) except the topologically distinctive phase in Fig. 2(c) (two crossing points).

The hypersensitive topological changes found by first-principles calculations demonstrate that the sliding motion creates interactions between effective non-Abelian $SU(4)$ gauge field background and massless fermions. In the presence of very tiny sliding, the nnn interlayer interaction (γ_3) is not constant any more but depends exponentially on the different pair distance between carbon atoms in top and bottom layers as shown in Fig. 1(d). The asymmetric inter-layer hopping interaction produces a constant pseudo-gauge potential in the terms of Hamiltonian containing γ_3 only, being similar with an effective Hamiltonian for strained SLG [24–26]. Hence, the effective Hamiltonian for sliding BLG can be written as,

$$\mathcal{H}'_{\text{eff}}(\vec{k}) = \hbar v_3 \vec{\tau} \cdot (\vec{k} - \vec{\lambda}) + \frac{\hbar v_3}{p_D} (\vec{\tau}^* \cdot \vec{k}) \tau_x (\vec{\tau}^* \cdot \vec{k}) \quad (1)$$

where $p_D \equiv \gamma'_1 v_3 / (\hbar v_0^2)$ and γ'_1 is the reduced nn inter-layer interaction. We find that the constant vector potential ($\vec{\lambda}$) explicitly depends on the sliding vector, $\vec{\lambda} \equiv (\lambda_x, \lambda_y) = \beta(d_y, -d_x)$ (β is estimated to be about $1/a_c$ from our first-principles calculations). The gauge symmetry in Eq. (1) apparently seems to be broken since $\vec{\lambda}$ is absent in the quadratic term. However, when we expand Eq. (1) at each Dirac point (\vec{k}_{Di}), the four Dirac cones shift depending on both $\vec{\lambda}$ and their own positions as $\vec{k}_{Di} \rightarrow \vec{k}_{Di} + \vec{A}_i(\vec{\lambda})$ ($i = 0, 1, 2, 3$). If $|\vec{\lambda}| \ll p_D$, $\vec{A}_0 = (\lambda_x, \lambda_y)$, $\vec{A}_1 = (-\lambda_x, \frac{\lambda_y}{3})$, $\vec{A}_2 = (-\frac{\sqrt{3}\lambda_y}{3}, -\frac{\sqrt{3}\lambda_x}{3} - \frac{2\lambda_y}{3})$ and $\vec{A}_3 = (\frac{\sqrt{3}\lambda_y}{3}, \frac{\sqrt{3}\lambda_x}{3} - \frac{2\lambda_y}{3})$. So, each Dirac cone moves along a different direction depending on its position.

An essential feature in the system that enables the ETT to occur is the shift of the four Dirac points along different directions under the sliding. To see this explicitly, we first assume that before sliding, there are four massless Dirac fermions, labeled by $i = 0, 1, 2, 3$, whose Hamiltonians are all isotropic and of same chirality: $\mathcal{H}_{Di} = \hbar v_3 \vec{\tau}^* \cdot \vec{\delta k}_i$ ($i = 0, 1, 2, 3$). We can then form a quadruplet out of four fermions, so that the index i is now viewed as the ‘color’ index of $SU(4)$ symmetry, and combine the four Hamiltonians \mathcal{H}_{Di} compactly as $\mathcal{H}_D = \hbar v_3 (\vec{\tau}^* \cdot \vec{\delta k}) \otimes \mathbf{I}$, where \mathbf{I} is the 4×4 identity matrix. If we now introduce the background gauge field $\vec{A} = (\mathbf{A}_x, \mathbf{A}_y)$ for the $SU(4)$ symmetry with $\mathbf{A}_x = \lambda_x \text{diag}(1, -1, 0, 0) - \frac{\lambda_y}{\sqrt{3}} \text{diag}(0, 0, 1, -1)$ and $\mathbf{A}_y = \frac{\lambda_x}{\sqrt{3}} \text{diag}(0, 0, -1, 1) + \lambda_y \text{diag}(1, \frac{1}{3}, -\frac{2}{3}, -\frac{2}{3})$ so that $\vec{\delta k} \mathbf{I} \rightarrow \vec{\delta k} \mathbf{I} - \vec{A}$ in the Hamiltonian, then \mathcal{H}_{Di} now becomes $\mathcal{H}_{Di} = \hbar v_3 \vec{\tau}^* \cdot (\vec{\delta k}_i - \vec{A}_i)$ ($i = 0, 1, 2, 3$) where \vec{A}_i are precisely the shifts of the Dirac points found in the previous paragraph. Since both \mathbf{A}_x and \mathbf{A}_y are linear combinations of the diagonal generators of $SU(4)$, we can now view the effect of sliding as creating a non-Abelian background gauge field. By a parity transformation for \mathcal{H}_{D0} and by anisotropic rescaling of $\vec{\delta k}_i$ for \mathcal{H}_{Di} ($i = 1, 2, 3$), we can transform the present model to the low energy Hamiltonian of BLG under sliding without altering \vec{A}_i .

The characteristics of the ETT are ruled by unique interplay between effective non-Abelian vector potential and conservation of Berry’s phase. In BLG, the Berry’s phase (ϕ_B) is 2π for a path enclosing the four Dirac points [5, 8]. For a path around each Dirac point, ϕ_B is $-\pi$ for the one at \vec{k}_{D0} and $+\pi$ for the other three at \vec{k}_{Di} ($i = 1, 2, 3$) [Fig. 3(a)]. So, the total ϕ_B is always conserved to be 2π [8]. Now, let’s first consider BLG sliding along $+\vec{\delta}_1$ direction [Figs. 2(c) and (d)], which corresponds to $\vec{\lambda} = (\lambda_x, 0) = \beta(-d_y, 0)$ ($d_y > 0$). In this case, we find that $\vec{A}_0 = -\vec{A}_1$ and $\vec{A}_2 = -\vec{A}_3$. Thus, the Dirac cones at \vec{k}_{D0} and \vec{k}_{D1} approach each other with sliding while those at \vec{k}_{D2} and \vec{k}_{D3} move away from each other [Fig. 3(b)]. The cones at \vec{k}_{D0} and \vec{k}_{D1} merge together when $\vec{\lambda} = (-p_D/4, 0)$ [Fig. 3(c)]. The

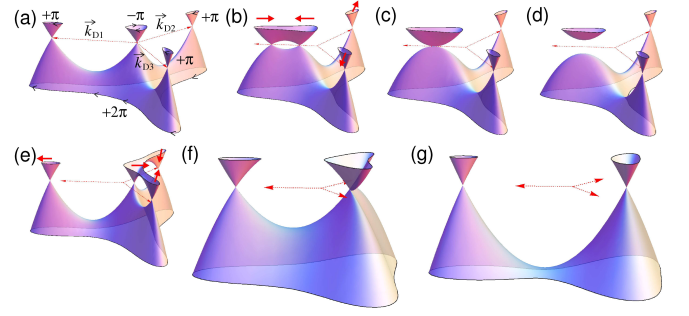


FIG. 3: Three dimensional plots of low energy bands from the effective Hamiltonian of Eq. (1) with $\vec{\lambda} = (\lambda_x, 0)$. (a) Without sliding ($\vec{\lambda} = 0$), three anisotropic Dirac cones with Berry phase π at \vec{k}_{Di} ($i = 1, 2, 3$) denoted by dotted red arrows in all panels, and isotropic one with $-\pi$ at \vec{k}_{D0} . Energy bands for sliding BLG with (b) $\lambda_x = -p_D/5$ (c) $-p_D/4$, (d) $-p_D/3$, (e) $p_D/5$, (f) $3p_D/4$ and (g) $1.8p_D$. The solid red arrows in (b) and (e) indicate the movements of Dirac cones at sliding.

corresponding sliding distance of d_y is about 0.3% of a_c ($d_y = p_D/(4\beta) \sim 0.004\text{\AA}$). For further sliding, the merged cone disappears and an energy gap develops as shown in Fig. 3(d). The gap is linear to sliding distance as given by $2\hbar v_3 \beta d_y \sim 0.9 \times [d_y/a_c]$ eV. The opening of energy gap signals a pair annihilation of two massless Dirac electrons with the opposite ‘topological charges’ of ± 1 . This also confirms the Berry’s phase conservation since remaining two anisotropic Dirac cones at \vec{k}_{D2} and \vec{k}_{D3} give the total ϕ_B of 2π . Next, we consider BLG sliding along $-\vec{\delta}_1$ direction ($\vec{\lambda} = (\lambda_x, 0) = \beta(d_y, 0)$) [Figs. 2(e) and (f)]. In this case, the three Dirac cones at \vec{k}_{D0} , \vec{k}_{D2} and \vec{k}_{D3} approach each other and remaining one at \vec{k}_{D1} moves away from them [Fig. 3(e)]. Those three cones merge together for sliding BLG with d_y about 1.2 % of a_c ($d_y = 3p_D/(4\beta) \sim 0.012\text{\AA}$) [Fig. 3(f)]. The merged cone has an anomalous dispersion [Fig. 3(f)] that gives the sickle-shaped energy contours as shown in Fig. 2(e). In contrast to the first case, no energy gap develops even when the sliding distance is increased further. Instead, the anomalous dispersion transforms to an anisotropic Dirac cone [Fig. 3(g)]. This phenomenon can be interpreted as a merging of two massless fermions of topological charge $+1$ with one of topological charge -1 . As a result, a new fermion of topological charge $+1$ is generated. We note that the total ϕ_B of 2π is conserved since the new particle has ϕ_B of π . Hence, the topological charges of fermionic particles in BLG are strictly governed by Berry’s phase conservation rule.

The direct signatures of the ETT can be readily measured using various experiment methods. We showed that the tiny sliding lifts the degeneracy at E_F as the number of Dirac cones is always reduced from four to two with significant increase of the saddle point energies and

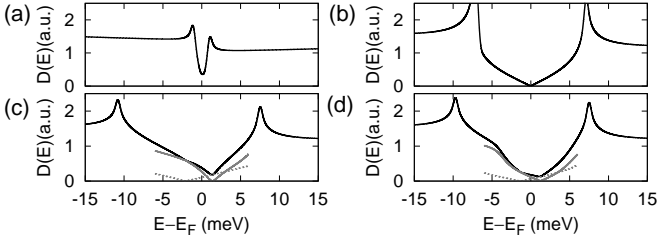


FIG. 4: First-principles calculations of total density of states of BLG $\vec{d}_s =$ (a) 0, (b) $0.02\vec{\delta}_1$, (c) $-0.02\vec{\delta}_1$, and (d) $0.012(\vec{\delta}_3 - \vec{\delta}_1)$. The grey solid and dotted lines in (c) and (d) are the partial density of states projected onto $\kappa_x > \kappa_s$ and $\kappa_x < \kappa_s$ region of the BZ in Fig. 2(e) and 2(g), respectively, where κ_s is a x -component of the saddle point of each energy contour.

deformations of remaining Dirac cones. Therefore, first, high-resolution scanning tunnelling microscopy [6, 27] can directly measure the changes in density of states ($D(E)$). Our first-principles calculations indeed show drastic variations in the position of van Hove singularity (vHS) below and above the charge neutral point upon sliding (Fig. 4). In between the two vHSs, the linear [Figs. 4(a) and (b)] or the mostly square-root dependence of $D(E)$ [Figs. 4(c) and (d)] appears as the sliding direction is changed, which is a unique feature of two-dimensional materials [28, 29]. Second, the Landau level (LL) spectrum for a small perpendicular magnetic field (B) also exhibits distinctive dependency on sliding direction. The atypical $D(E) \sim \sqrt{E}$ for BLG with sliding along $\vec{d}_s = -0.02\vec{\delta}_1$ and $0.012(\vec{\delta}_3 - \vec{\delta}_1)$ produces an LL spectrum of $E_n \sim \pm(Bn)^{2/3}$ (n , non-negative integer). On the other hand, for BLG with a sliding along $\vec{d}_s = 0.02\vec{\delta}_1$, $D(E) \sim |E|$ gives $E_n \sim \pm(Bn)^{1/2}$. Third, a minimal conductivity of $24e^2/(\pi^2\hbar)$ at the charge neutral point [10–12] will decrease quickly when sliding occurs (e is the electron charge). For example, for sliding BLG with $\vec{d}_s = -0.1\vec{\delta}_1$ [Fig. 2(f)], we find that the conductivity decreases to $\sim 8e^2/(\pi^2\hbar)$.

Finally, we discuss the role of the smallest interlayer interaction γ_4 [Fig. 1(e)]. It adds an additional small term $2\hbar^2 v_0 v_4 \vec{k} \cdot (\vec{k} + \vec{\lambda})/\gamma_1$ to Eq. (1) where $v_4 = (3/2)\gamma_4 a_c/\hbar$. Without sliding, this contributes a tiny difference ($\sim 10^{-4}\gamma_0$) in Dirac energies between hole- and the electron-doped cones [Fig. 2(b)]. When BLG slides along $-\vec{\delta}_1$ direction with $d_y > 0.01a_c$, this term turns the hole-doped cone into the electron-doped and vice versa, and increases the amount of doping linearly with sliding distance [Figs. 2(e)-(h)]. However, γ_4 does not affect any topological changes discussed so far.

In summary, we show that the topology of energy bands of BLG changes significantly if sliding occurs. Hence, the ETT driven by non-Abelian gauge fields that are thought to be possible in cold atomic gas [28–30] or similar effects in high energy physics [31] can be readily

realizable in sliding BLG.

Y.-W.S. acknowledges discussions with K. Lee, P. Yi, and K. Novoselov. Y.-W.S. was supported by the NRF grant funded by the Korea government (MEST) (QMMRC, No. R11-2008-053-01002-0 and Nano R&D program 2008-03670). S.-M.C. and S.-H.J. were supported by NRF funded by MEST (Grant 2009-0087731 and WCU program No. R31-2008-000-10059-0).

* Electronic address: hand@kias.re.kr

† Electronic address: jhish@postech.ac.kr

- [1] I. M. Lifshitz, Sov. Phys. JETP **21**, 1130 (1960).
- [2] Y. M. Blanter *et al.*, Phys. Rep. **245**, 159 (1994).
- [3] A. A. Varlamov, V. S. Egorov, and A. V. Patsulaya, Adv. Phys. **38**, 469 (1989).
- [4] N. P. Armitage *et al.*, Phys. Rev. Lett. **104**, 237401 (2010).
- [5] K. S. Novoselov *et al.*, Nat. Phys. **2**, 177 (2006).
- [6] G. Li *et al.*, Nat. Phys. **6**, 109 (2009).
- [7] B. E. Feldman, J. Martin, and A. Yacoby, Nat. Phys. **5**, 889 (2009).
- [8] Y. Lemonik *et al.*, Phys. Rev. B **82**, 201408 (2010).
- [9] E. McCann and V. I. Fal'ko, Phys. Rev. Lett. **96**, 086805 (2006).
- [10] M. Koshino and T. Ando, Phys. Rev. B **73**, 245403 (2006).
- [11] J. Nilsson *et al.*, Phys. Rev. B **78**, 045405 (2008).
- [12] J. Cserti, A. Csordás, and G. Dávid, Phys. Rev. Lett. **99**, 066802 (2007).
- [13] H. Min *et al.*, Phys. Rev. B **75**, 155115 (2007).
- [14] A. H. Castro Neto *et al.*, Rev. Mod. Phys. **81**, 109 (2009).
- [15] J. M. B. Lopes dos Santos, N. M. R. Peres, and A. H. Castro Neto, Phys. Rev. Lett. **99**, 256802 (2007).
- [16] S. Shallcross, S. Sharma, and O. A. Pankratov, Phys. Rev. Lett. **101**, 056803 (2008).
- [17] J. Hass *et al.*, Phys. Rev. Lett. **100**, 125504 (2008).
- [18] P. Giannozzi *et al.*, J. Phys.:Condens. Matter **21**, 395502 (2009).
- [19] J. P. Perdew, K. Burke, and M. Ernzerhof, Phys. Rev. Lett. **77**, 3865 (1996).
- [20] S. Grimme, J. Comput. Chem. **27**, 1787 (2006).
- [21] V. Barone *et al.*, J. Comput. Chem. **30**, 934 (2008).
- [22] A. N. Kolmogorov and V. H. Crespi, Phys. Rev. Lett. **85**, 4727 (2000).
- [23] A. B. Kuzmenko *et al.*, Phys. Rev. B **80**, 165406 (2009).
- [24] V. M. Pereira, A. H. Castro Neto, and N. M. R. Peres, Phys. Rev. B **80**, 045401 (2009).
- [25] S.-M. Choi, S.-H. Jhi, and Y.-W. Son, Phys. Rev. B **81**, 081407 (2010).
- [26] F. Guinea, M. I. Katsnelson, and A. K. Geim, Nat. Phys. **6**, 30 (2010).
- [27] Y. J. Song *et al.*, Nature **467**, 185 (2010).
- [28] G. Montambaux *et al.*, Phys. Rev. B **80**, 153412 (2009).
- [29] B. Wunsch, F. Guinea, and F. Sols, New. J. Phys. **10**, 103027 (2008).
- [30] A. Bermudez *et al.*, New. J. Phys. **12**, 033041 (2010).
- [31] Y. Hosotani, Phys. Lett. **129B**, 193 (1983).